Regenerative Therapy 21 (2022) 1–8

Contents lists available at ScienceDirect

Regenerative Therapy

journal homepage: http://www.elsevier.com/locate/reth

Original Article

# Downregulated HDAC3 or up-regulated microRNA-296-5p alleviates diabetic retinopathy in a mouse model

Songtian Che [a], Shuai Wu [b], Peng Yu [a, *]

[a] Department of Ocular Fundus Disease, the Second Hospital of Jilin University, No. 4026, Yatai Street, Changchun 130041, Jilin, People's Republic of China
[b] Department Orbital Diseases & Ocular Plastic Surgery, the Second Hospital of Jilin University, No. 4026, Yatai Street, Changchun 130041, Jilin, People's Republic of China

ARTICLE INFO

*Article history:*
Received 20 February 2022
Received in revised form
2 April 2022
Accepted 14 April 2022

*Keywords:*
Diabetic retinopathy
Histone deacetylase 3
MicroRNA-296-5p
G protein subunit alpha i2
Apoptosis
Retinal ganglion cells

ABSTRACT

*Objective:* It has been demonstrated the efficacy of histone deacetylase 3 (HDAC3) in diabetes. Nevertheless, the function of HDAC3 in diabetic retinopathy (DR) remained largely obscure. Here, we investigated the HDAC3 effects in DR mice through the microRNA (miR)-296-5p/G protein subunit alpha i2 (GNAI2) axis.

*Methods:* The mice diabetes model was established. HDAC3, GNAI2 and miR-296-5p levels in retina tissues of DR mice were evaluated. The weight, blood glucose, Evans blue leakage in DR mice, apoptosis of retinal ganglion cells, vascular endothelial growth factor (VEGF) and malondialdehyde (MDA) contents and superoxide dismutase (SOD) activity in DR mice were detected after miR-296-5p elevation or HDAC3 depletion. The relations among HDAC3, miR-296-5p and GNAI2 were validated.

*Results:* HDAC3 and GNAI2 expressed at a high level while miR-296-5p expressed at a low level in retina tissues of DR mice. Restoring miR-296-5p or depleting HDAC3 reduced Evans blue leakage in DR mice, attenuated apoptosis of retinal ganglion cells, reduced VEGF and MDA, and enhanced SOD activity in serum and retinal tissues of DR mice. HDAC3 repressed miR-296-5p expression by binding to its promoter region, thereby enhancing GNAI2 expression.

*Conclusion:* Depleting HDAC3 or restoring miR-296-5p suppresses apoptosis of retinal ganglion cells of DR mice via down-regulating GNAI2.



## 1. Introduction

Diabetic retinopathy (DR) is a fundamental microvascular complication that induces vision-threatening retinal changes in one-third of diabetics [1]. DR is featured by progressive changes in the retinal microvasculature, resulting in raised vasopermeability, retinal non-perfusion, and pathologic intraocular proliferation of retinal vessels [2]. The risk factors for the development of DR include hyperglycemia, hyperlipidemia, hypertension and smoking [3]. Current therapeutic strategies for DR include the anti-vascular endothelial growth factor (VEGF) drug treatment, retinal laser photocoagulation, steroids treatment and surgical treatment [4]. The molecular mechanism of the complex blinding disease is still not clear [5]. Although advancement has been made in the diagnosis of DR, early diagnosis of DR remains challenging, resulting in poor treatment outcomes [6]. The austere fact of DR makes it necessitated to probe novel therapeutic modalities for DR patients.

Histone deacetylase (HDAC) family is a key epigenetic modulator that control gene expression through deacetylation of transcription and histones factors [7]. It is revealed that down-regulated HDAC3 prevents blood-brain barrier permeability in type 2 diabetes male mice [8]. A previous study has contended that HDAC3, as a new mechanism for kidney injury, provides a potential therapeutic target for type 2 diabetes [9]. Also, HDAC3 is dynamically expressed in retinal ganglion cells in DR, which is associated with cellular apoptosis and autophagy [10]. MicroRNAs (miRNAs) are a series of endogenous ncRNAs that suppress downstream target genes expression via post-transcriptional modulation [11]. MiR-296-5p is dysregulated in tissue samples of diabetes mellitus

* Corresponding author. Peng Yu Department of Ocular Fundus Disease, the Second Hospital of Jilin University, No. 4026, Yatai Street, Changchun 130041, Jilin, People's Republic of China. Tel: +0431-81136535
*E-mail address:* YuPeng535@163.com (P. Yu).

Peer review under responsibility of the Japanese Society for Regenerative Medicine.

https://doi.org/10.1016/j.reth.2022.04.002

patients [12]. In addition, miR-296-5p is diminished in patients with high glucose, which is a complication of diabetes mellitus [13]. In addition to that, the bioinformatics website predicted the binding sits of miR-296-5p and G protein subunit alpha i2 (GNAI2). As a heterotrimeric G-protein subunit, GNAI2 modulates multiple cell functions, such as ion channel activity and various cell activities [14,15]. Furthermore, GNAI2 deficiency has been manifested to alleviate the major cause of diabetes– diet-induced obesity [16] As for DR, GNAI2 has been reported to be involved in the antioxidant activity, acting like a candidate for DR treatment [17]. Given the former analyses, HDAC3 functioned as a pivotal modulator in the progression of diabetes, while the regulatory mechanism of the HDAC3/miR-296-5p/GNAI2 axis in DR remained obscure. Therefore, this study was dedicated to expected to further unraveling the impacts of HDAC3, miR-296-5p and GNAI2 in DR mice, thus affording novel therapeutic targets for DR treatment.

## 2. Materials and methods

### 2.1. Ethics statement

Animal experiments were processed under the supervision of the Institutional Animal Care Use Committee of the Second Hospital of Jilin University.

### 2.2. Experiment animals

C57BL/6 male mice of specific pathogen-free grade (18—22 g, animal center of Jilin university, Jilin, China) were obtained. Mice were adaptively fed for 1 w with water and food at (22 ± 1)°C with (55 ± 5)% humidity and 12 h day/night cycle [18].

### 2.3. Establishment of a mouse model of type I diabetes mellitus and grouping

Citric acid and sodium citrate (0.1 M) solution were mixed with a proportion of 14 : 11 (pH = 4.2—4.5) and prepared into streptozotocin (STZ) dissolution buffer. STZ powder was dissolved in buffer and placed on ice avoiding light. Mice were fasted for 12 h, then given intraperitoneal injection of STZ at 50 $mg \cdot kg^{-1}$ and continuously injected for 5 d. Mice in the normal group were intraperitoneally injected with the same volume of buffer. After 1 w of modeling, blood samples were obtained from the tail vein to assess the blood glucose concentration, and the level of blood glucose above 16.7 $mmoL^{-1}$ was considered as a successful diabetes model [19].

Group classification was performed randomly divided into 7 groups (14 mice in each group): small hairpin RNA (sh)-HDAC3 group (injection of sh-HDAC3 in the vitreous body), sh-negative control (NC) group (injection of sh-HDAC3 NC in the vitreous body), miR-296-5p agomir group (injection of miR-296-5p agomir in the vitreous body), agomir NC group (injection of miR-296-5p agomir NC in the vitreous body), sh-HDAC3 + miR-296-5p antagomir group (injection of sh-HDAC3 and miR-296-5p antagomir in the vitreous body) and sh-HDAC3 + antagomir NC group (injection of sh-HDAC3 and miR-296-5p antagomir NC in the vitreous body). Intravitreal injections were performed during the first week after diabetes induction. We injected various constructs (sh-HDAC3, miR-296-5p agomir, miR-296-5p antagomir and NC) into the corresponding mouse vitreou by using the 30-gauge needle (Becton, Dickinson and Company. Franklin Lakes, NJ, USA.). The injection was conducted in both eyes and repeated twice a week until nine injections were completed. Mice without any treatment were set in the control group [10].

### 2.4. Evans blue staining

Tweenty weeks after the DM model, 6 mice in each group were intraperitoneally injected with 10 μL/g Evans blue which was dissolved in phosphate-buffered saline (PBS). After 2 h, normal saline (37 °C) was perfused into the left ventricular to remove the Evans blue in the systemic circulation of mice. Then the eyeballs of mice were taken, and the retinal tissues were cut off under the dissecting microscope, dried in the vacuum drying oven at 55 °C for 5 h and weighed. The tissues were added with 120 μL formamide (Sigma-Aldrich, SF, CA, USA), water bathed (70 °C) for 18 h to extract Evans blue. The extract solution was centrifuged for 1 h at 10,000×*g*, the supernatant (60 μL) was absorbed to examine the optical density value at 620 nm on a microplate reader. The value was substituted to the standard curve to calculate the amount of Evans blue. The ratio of the amount of Evans blue to the weight of dried retinal tissues was calculated [20].

### 2.5. Hematoxylin-eosin (HE) staining

Retinal tissues were fixed in 4% paraformaldehyde, embedded by paraffin, dewaxed, rehydrated and sliced to 5 μm sections. Staining was performed using the HE staining kit (Solarbio, Beijing, China) to detect the pathological traits in the retinal tissues [10]. The slides were blocked with neutral gum, and were then transferred to a microscope to observe the staining effect. The morphological structure of retinal cells and the changes in the ganglion cell layer were observed under a Zeiss optical microscope (Zeiss AG, Oberkochen, Germany) with a magnification of 400 times. The ganglion cell count was the average number of ganglion cells seen per high-power microscope.

### 2.6. Terminal deoxynucleotidyl transferase-mediated deoxyuridine triphosphate-biotin nick end labeling (TUNEL) staining

TUNEL staining was implemented with the In Situ Cell Death Detection Kit following the manufacturer's requirements (KeyGEN, China). The mouse retinal tissue sections were then stained with DAPI (a nuclear-specific marker), and captured with a confocal microscope (Zeiss) to analyze the apoptosis in the retinal tissues of each group of mice [21].

### 2.7. Reverse transcription quantitative polymerase chain reaction (RT-qPCR)

The RNeasy Mini Kit (Qiagen, Valencia, CA, USA) was employed for RNA extraction. For mRNA detection, the complementary DNA (cDNA) was obtained by PrimeScriptTM RT reagent kit with gDNA Eraser (Takara Bio Inc.). miRNA were polyadenylated by poly(A) polymerase and reverse transcribed to cDNA using the One Step PrimeScript® miRNA cDNA Synthesis Kit (TaKaRa, China). The SYBR® Premix Ex TaqTM II (Perfect Real Time) kit (Takara) was employed for loading. Samples were processed with RT-qPCR in a real-time fluorescence PCR instrument (ABI 7500, ABI, Foster City, CA, USA). The β-actin and U6 were set as endogenous references (primer sequences were exhibited in Supplementary Table 1). The gene levels were detected using the $2^{-\Delta\Delta Ct}$ method.

### 2.8. Western blot analysis

The total protein extraction in the retinal tissues was performed. The protein concentration was determined by the bicinchoninic acid method. The protein was performed sodium dodecyl sulfate polyacrylamide gel electrophoresis and transferred to the polyvinylidene fluoride membrane. The membrane was added with

blocking liquid for 1 h, following incubation with primary antibodies HDAC3 (1 : 1000, Abcam), GNAI2 (1 : 2000, Abcam), and then incubated with corresponding secondary antibody for 1 h. The membrane was developed by BeyoECL Plus chemiluminescence solution (Beyotime). The results were pictured by a FluorChem8000 imager (Alpha Innotech., San Leandro, CA, USA), and the AlphaEaseFC 4.0 software was applied for gray value analysis.

### 2.9. Enzyme-linked immunosorbent assay (ELISA)

The whole blood was placed for 2 h, centrifuged for 15 min at 4 °C, 2000 g to isolate the supernatant. The retina was mixed with 400 μL whole protein lysate (Sigma) and added with protease inhibitor. Then, the lysate was centrifuged for 15 min at 4 °C, 12,000 g to take the supernatant. The contents of VEGF, superoxide dismutase (SOD) and malondialdehyde (MDA) in serum and tissues were detected according to the corresponding kit instructions [22].

### 2.10. Chromatin immunoprecipitation (ChIP) assay

HDAC3 levels in the miR-296-5p promoter region were assessed using a ChIP kit (Millipore, Boston, MA, USA). Mouse retinal microvascular endothelial cells (mRMECs) at the logarithmic growth phase were subjected to 10-min fixation with 1% formaldehyde for DNA-protein crosslink formation. Cells were treated with sonicate and centrifugation at 13,000 rpm at 4 °C. The supernatant was obtained and divided into three tubes. IgG and antibody HDAC3 (1:1000, Abcam) was added and followed by overnight incubation at 4 °C. Afterwards, protein agarose or agarose was adopted to precipitate the endogenous DNA-protein complexes and then centrifuged and the supernatant discarded. The retained complexes were subjected to cross-link overnight at 65 °C. DNA fragments were obtained by phenol/extraction and purification. The INPUT was set as the endogenous reference. The promoter region-specific primer miR-296-5p was adopted to assess the binding between HDAC3 and miR-296-5p [23,24].

### 2.11. Dual luciferase reporter gene assay

The relation between miR-296-5p and GNAI2 together with miR-296-5p and GNAI2 3'untranslated region (UTR) was predicted by the bioinformatics website (https://starbase.sysu.edu.cn). The 3′UTR sequences of GNAI2 and its corresponding mutant (MUT) 3′UTR sequences were cloned into the pmiR-RB-Report™ vector (RIBOBIO, Guangzhou, China). mRMECs were seeded on a 24-well plate at 4 × $10^5$ cells/well. The luciferase reporter gene, renilla luciferase plasmid pRL-TK and miRNA were co-transfected into mRMECs with Lipofectamine2000. After 48 h, cells were lysed by

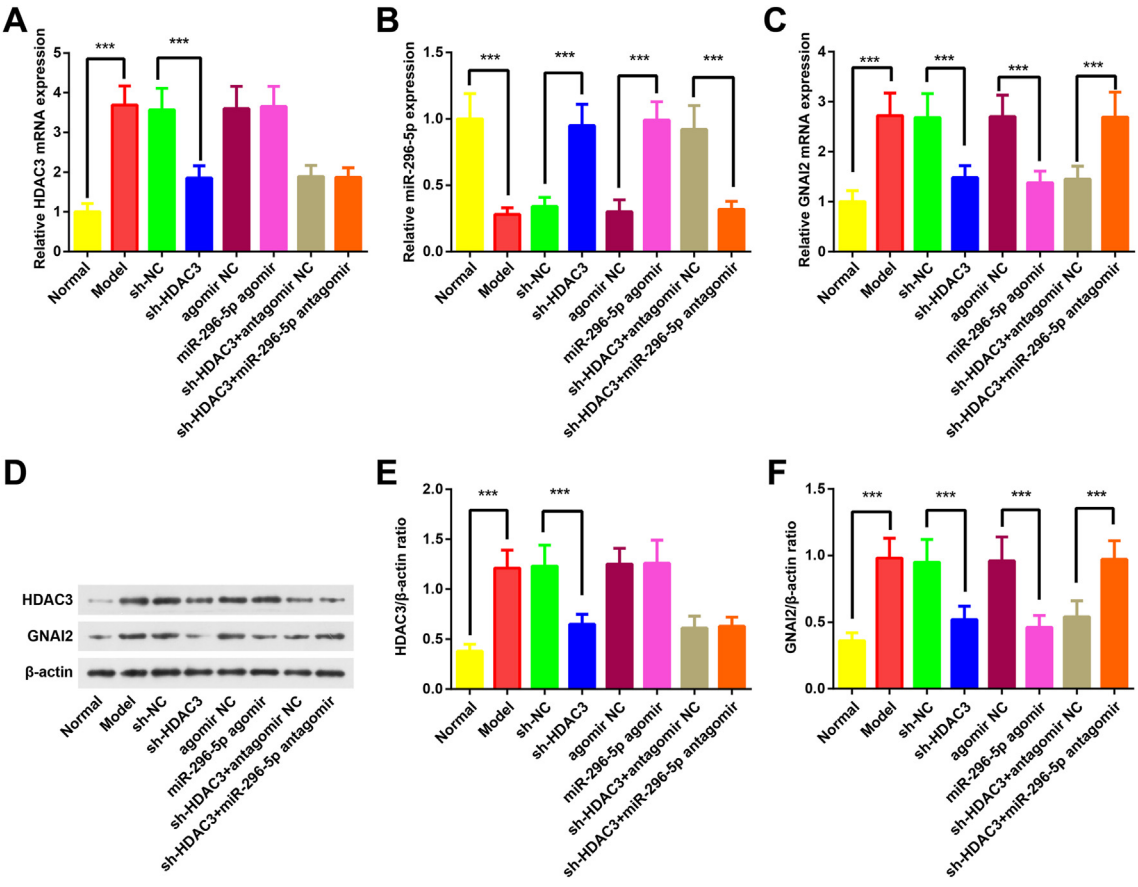


**Fig. 1.** HDAC3 and GNAI2 are raised while miR-296-5p is reduced in retinal tissues of DR mice. A, HDAC3 mRNA expression in retinal tissues of mice. B, miR-296-5p expression in retinal tissues of mice. C, GNAI2 mRNA expression in retinal tissues of mice. D, Protein bands of HDAC3 and GNAI2 in retinal tissues of mice. E, HDAC3 protein expression in retinal tissues of mice. F, GNAI2 protein expression in retinal tissues of mice. ***$P < 0.001$. Measurement data were indicated as mean ± standard deviation. Comparisons among multiple groups were assessed by ANOVA followed by Tukey's post hoc test.

lysate, then added with LAR II. The fluorescence value M1 was obtained by a luminometer. Renilla luciferase detection was performed by Stop&Glo detection liquid, and fluorescence value M2 was obtained. The luciferase activity of the reporter gene was M1/M2 [25].

### 2.12. Statistical analysis

All data were analyzed by SPSS 21.0 software. Measurement data were indicated by mean ± standard deviation. The *t*-test was adopted for a two-group data comparison. The analysis of variance (ANOVA) and Tukey's post hoc test were employed for data comparisons among multiple groups. *P* value < 0.05 suggested significant statistical difference.

## 3. Results

### 3.1. HDAC3 and GNAI2 are elevated while miR-296-5p is depleted in retina tissues of DR mice

RT-qPCR and Western blot analysis revealed that HDAC3 and GNAI2 mRNA and protein levels were elevated while miR-296-5p was reduced in retina tissues in the DR mice. HDAC3 and GNAI2 mRNA and protein expression were reduced while miR-296-5p was elevated in retina tissues in DR mice treated with sh-HDAC3. GNAI2 levels were depleted and miR-296-5p was enhanced in retina tissues in DR mice after being injected with miR-296-5p agomir (Fig. 1A–F). The findings presented that HDAC3 and GNAI2 were raised while miR-296-5p was reduced in retinal tissues of DR mice.

### 3.2. Restoring miR-296-5p or depleting HDAC3 reduces Evans blue leakage and increases ganglion cells in DR mice

First, we analyzed the changes in body weight and blood glucose of the mice in each group. The blood glucose results revealed (Fig. 2A and B) that the blood glucose of mice was elevated in the other groups in comparison to the normal group, and the blood glucose values were all higher than 16.7 mmol·L$^{-1}$, implying that we successfully established the diabetes model. Additionally, the determination of body weight demonstrating that compared with the normal group, mice in the other groups displayed lower body weight. Further analysis of all the model groups uncovered that mice injected with sh-HDAC3 and miR-296-5p agomir exhibited increased body weight.

The Evans Blue leak method detected the vascular permeability in DR mice. The results of retinal Evans blue leakage detection uncovered that the Evans blue leakage was augmented in the DR mice. The Evans blue leakage was decreased in DR mice after injection of sh-HDAC3 or miR-296-5p agomir. Moreover, the Evans blue leakage was enhanced in DR mice injected with the sh-HDAC3 + miR-296-5p antagomir compared to injected with the sh-HDAC3 + antagomir NC (Fig. 2C).

The results of HE staining (Fig. 2D and E) revealed that the retinal tissues of the normal mice were clear and intact, and the retinal ganglion cells were arranged in a single layer with a complete morphology and numerous cells. The number of ganglion cells was elevated in DR mice treated with sh-HDAC3 or miR-296-5p, while ganglion cells were diminished in DR mice treated with sh-HDAC3 + miR-296-5p antagomir compared to injected with the sh-HDAC3 + antagomir NC.

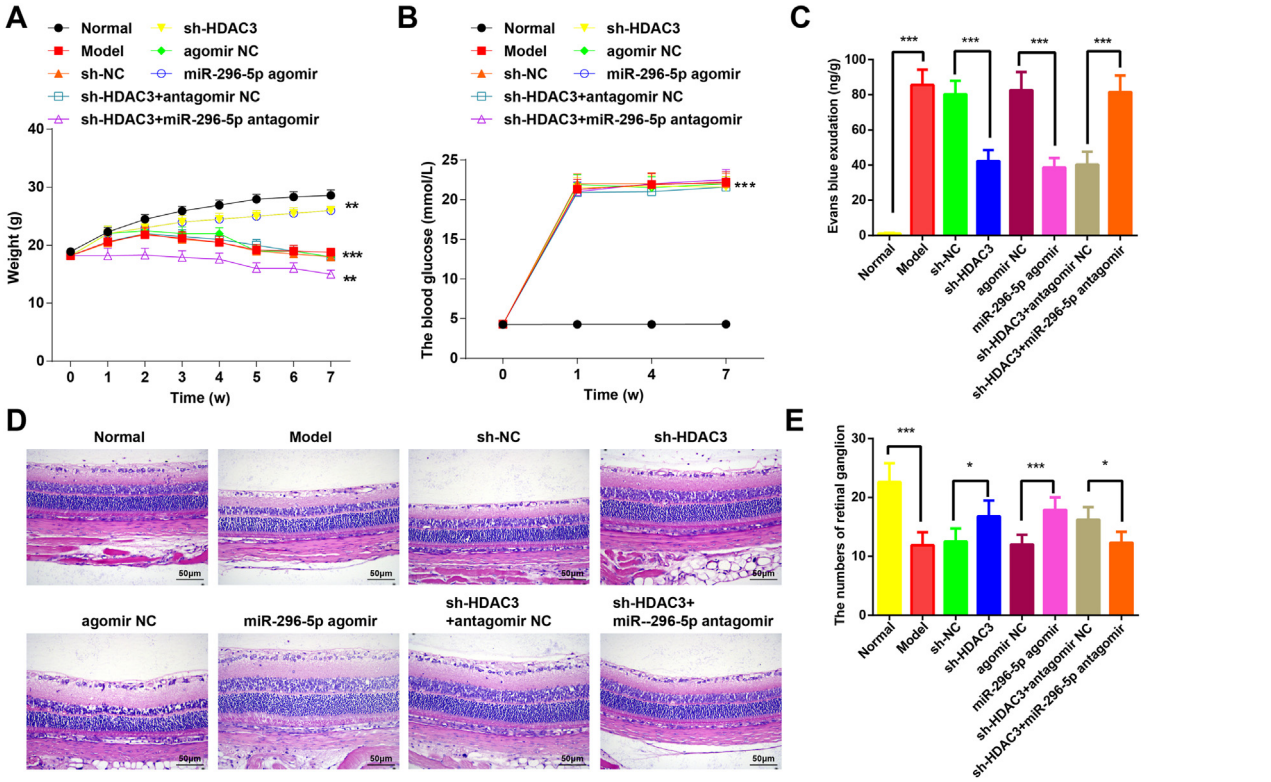


**Fig. 2.** Restoring miR-296-5p or depleting HDAC3 reduces Evans blue leakage in DR mice. A, The change of mice weight. B, The change of blood glucose in mice. C, Evans blue leakage in mice of each group. D. The change of histological damage was detected by HE staining; E, Number of retinal ganglion cells in each group of mice. *$P$ < 0.05, **$P$ < 0.01; ***$P$ < 0.001. Measurement data were indicated as mean ± standard deviation. Comparisons among multiple groups were assessed by ANOVA followed by Tukey's post hoc test.

The discoveries summarized that restoring miR-296-5p or depleting HDAC3 reduced Evans blue leakage and increased ganglion cells in DR mice.

### 3.3. Elevated miR-296-5p or depleted HDAC3 attenuates apoptosis in retinal tissues of DR mice

TUNEL staining results (Fig. 3A–E) presented that TUNEL positive cell rate was heightened in retinal tissues in DR mice, which also displayed lower Bcl-2 expression and higher Bax and Caspase-3 expression. After injection of sh-HDAC3 or miR-296-5p agomir, TUNEL positive cell rate was decreased, accompanied with reduced Bax and Caspase-3 expression and elevated Bcl-2 expression. In DR mice after sh-HDAC3 + miR-296-5p antagomir injection, the TUNEL positive cell rate was enhanced, Bax and Caspase-3 expression was raised and Bcl-2 expression was reduced compared to injected with the sh-HDAC3 + antagomir NC. The results exhibited that overexpressed miR-296-5p or silencing HDAC3 attenuated apoptosis in retinal tissues of DR mice.

### 3.4. Increased miR-296-5p or silencing HDAC3 reduces VEGF and MDA contents and enhances SOD activity in serum and retinal tissues of DR mice

VEGF, MDA and SOD levels were tested in retinal tissues and serum of DR mice. The results suggested VEGF and MDA contents were enhanced and SOD activity was decelerated in DR mice. Nevertheless, after injection of sh-HDAC3 or miR-296-5p agomir, VEGF and MDA contents were depleted and SOD activity was enhanced in DR mice. In mice injected with sh-HDAC3 + miR-296-5p antagomir, VEGF and MDA contents were heightened and SOD activity was reduced in DR mice in comparison to injected with the sh-HDAC3 + antagomir NC (Fig. 4A–F). The outcomes implicated that miR-296-5p augmentation or HDAC3 deficiency reduced VEGF expression and repressed oxidative stress of DR mice.

### 3.5. HDAC3 targets miR-296-5p to modulate GNAI2 levels

miR-296-5p was reported to inhibit the development of diabetes [12]. Therefore, we hypothesized that HDAC3 might interact with miR-296-5p. For verification purpose, the expression of miR-296-5p was evaluated when HDAC3 was upregulated and downregulated, respectively. The results indicated that there was a negative correlation between HDAC3 and miR-296-5p expression (Fig. 5A,B). Next, as for the effect of HDAC3 on the promoter activity of miR-296-5p, the ChIP-qPCR experiment was performed and the results uncovered that the promoter activity of miR-296-5p was deteriorated when HDAC3 was upregulated (Fig. 5C).

The binding of miR-296-5p and GNAI2 was predicted by the bioinformatics website (https://starbase.sysu.edu.cn) (Fig. 5D). The dual luciferase reporter gene assay further revealed that (Fig. 5E) after co-transfection of miR-296-5p mimic or mimic NC with the GNAI2 reporter gene, the luciferase activity of cells upon treatment of miR-296-5p mimic was reduced. Thus, miR-296-5p could inhibit the luciferase activity of GNAI2 reporter gene, indicating that miR-296-5p was bound to GNAI2 3′UTR. The outcomes validated that GNAI2 was the target gene of miR-296-5p. These discoveries

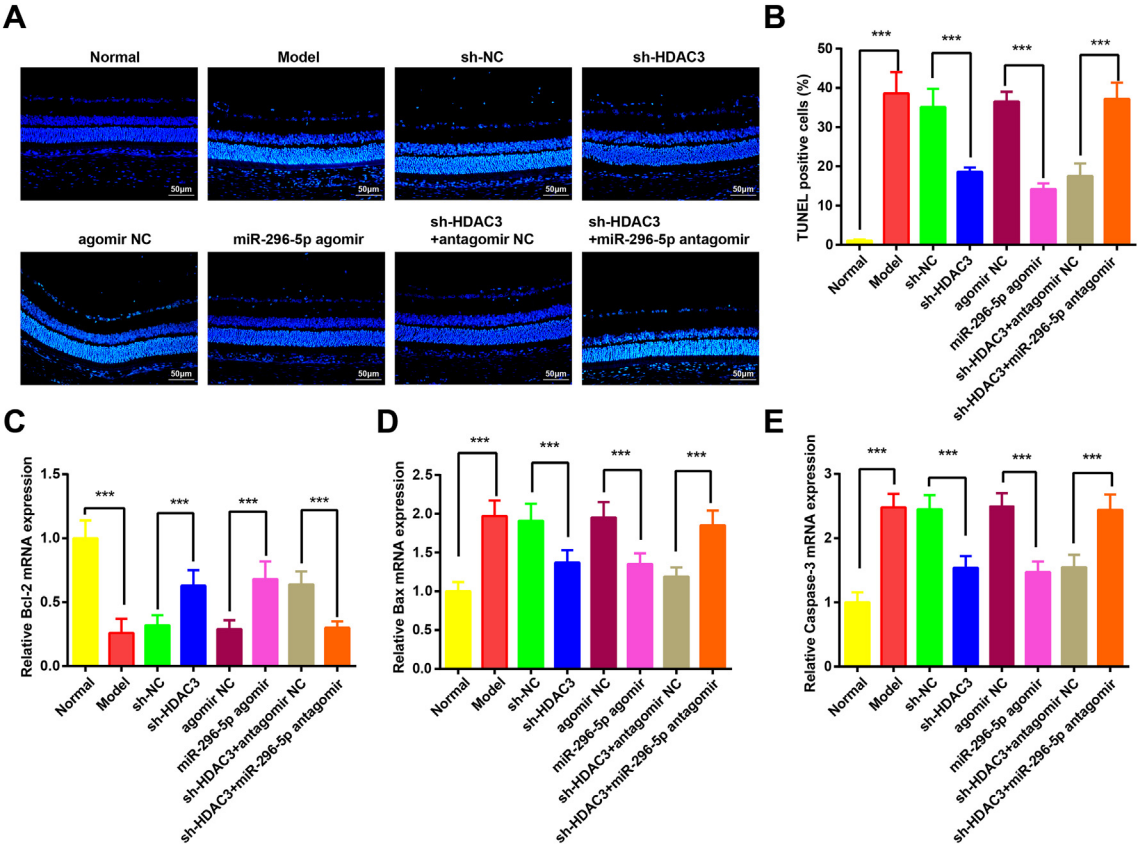


**Fig. 3.** Enhanced miR-296-5p or depleted HDAC3 attenuates apoptosis in retinal tissues of DR mice. A, TUNEL staining of retinal tissues in mice. B, TUNEL positive cell rate in retinal tissues of mice. C-E, Bcl-2, Bax and Caspase-3 mRNA expression was detected using RT-qPCR. ***$P < 0.001$. Measurement data were indicated as mean ± standard deviation. Comparisons among multiple groups were assessed by ANOVA followed by Tukey's post hoc test.

evidenced that HDAC3 repressed miR-296-5p expression by binding to its promoter region, thereby enhancing GNAI2 expression.

## 4. Discussion

DR is a primary inducer for blindness in working-age people globally [26]. In an article conducted by Zhang et al., it is elucidated that depletion of HDAC3 in diabetic mice prevents diabetes-induced liver damage [27]. Also, recent literature has indicated that miR-296-5p is expressed in tissue samples of diabetes mellitus patients [12,28]. It is customarily considered that the placental growth factor may be a potential guardian against insulin resistance, and likely through depleting the GNAI2, which may offer insight for future therapeutic approaches for treating DR [17,29]. The current study was conducted to explore the roles of HDAC3, miR-296-5p and GNAI2 in DR mice.

In this research, it was of particular interest that HDAC3 and GNAI2 were raised while miR-296-5p was reduced in retinal tissues of DR mice. It has been uncovered that HDAC3 activity is markedly elevated in the heart of diabetic mice [30]. Consistently, HDAC3 expression has also been validated to be heightened in diabetic mice with cerebral ischemia/reperfusion (I/R) [31]. As for miR-296-5p expression, it has been manifested that miR-296-5p levels are remarkably down-regulated in patients with type 1 diabetes mellitus [24]. Similarly, Favaro et al. have elucidated that miR-296-5p also displayed a low level in patients with high glucose that induces diabetes mellitus [13,32]. Concerning GNAI2, elevated GNAI2 level has been confirmed in diabetes-accelerated atherosclerosis, and mutant GNAI2 can abrogate the effects of GNAI2-CXCR5 coupling on alleviating atherosclerosis in diabetic mice [33]. In addition, our study revealed that GNAI2 was the target gene of miR-296-5p, but scarcely any study has discussed the relation between miR-296-5p and GNAI2 in DR, even between miRNAs and GNAI2.

Additionally, we observed that the body weight of mice was decreased while blood glucose and Evans blue leakage were raised in mice with DR. As reported, STZ intraperitoneal injection into mice exhibited lower body weight and hyperglycemia, which is commonly found in STZ-induced diabetic mice [34]. A study has presented that blood glucose, retinal cell apoptosis, the number of active caspase-3-positive cells, MDA level are raised while body weight and SOD activity are decreased in rats in the diabetes mellitus [35]. It has been revealed that the Evans blue leakage is decreased in the diabetic models [36]. Moreover, it was reported by our study that restoring miR-296-5p or depleting HDAC3 increased the number of retinal ganglion cells, attenuated TUNEL positive cell

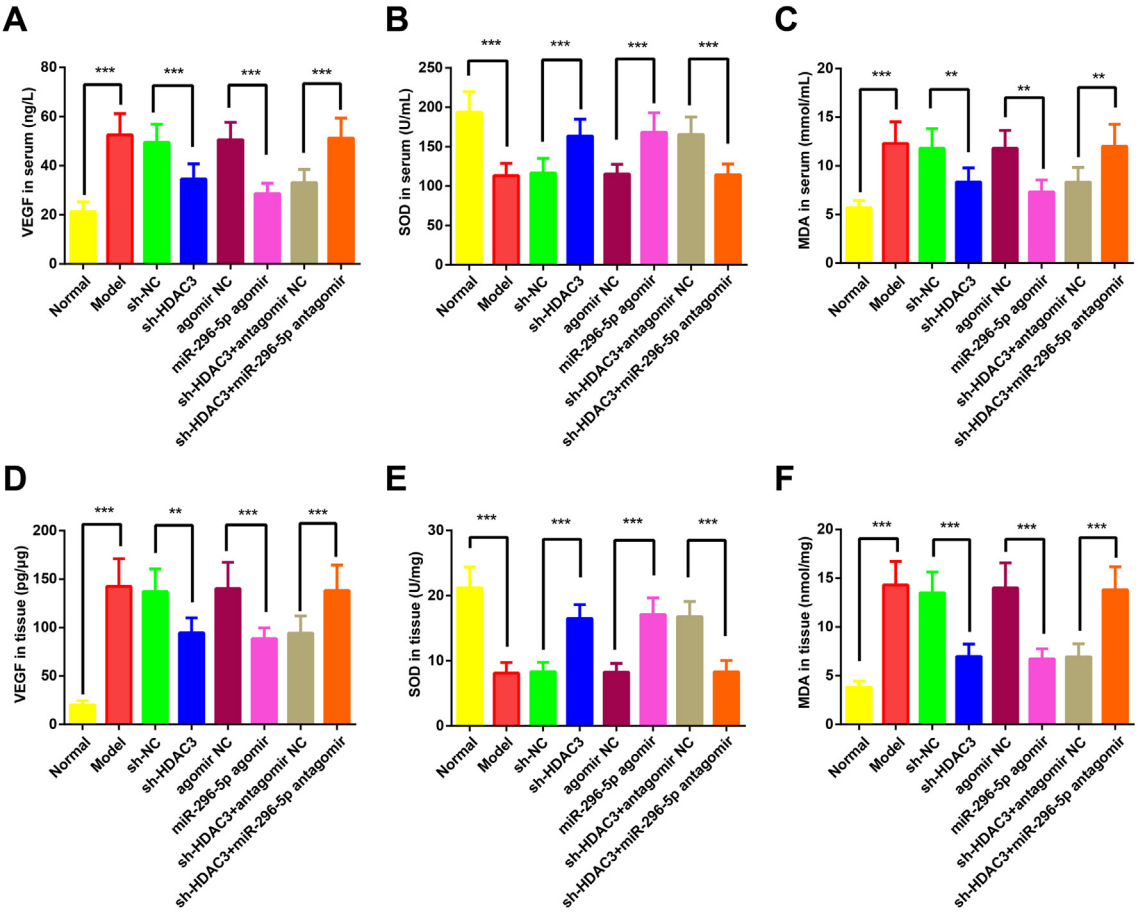


**Fig. 4.** Elevated miR-296-5p or silenced HDAC3 reduces VEGF and MDA contents as well as enhances SOD activity in serum and retinal tissues of diabetes mice. A, VEGF content in serum of mice. B, SOD activity in serum of mice. C, MDA content in serum of mice. D, VEGF content in retinal tissues of mice. E, SOD activity in retinal tissues of mice. F, MDA content in retinal tissues of mice. $^{**}P < 0.01$; $^{***}P < 0.001$. Measurement data were indicated as mean ± standard deviation. Comparisons among multiple groups were assessed by ANOVA followed by Tukey's post hoc test.

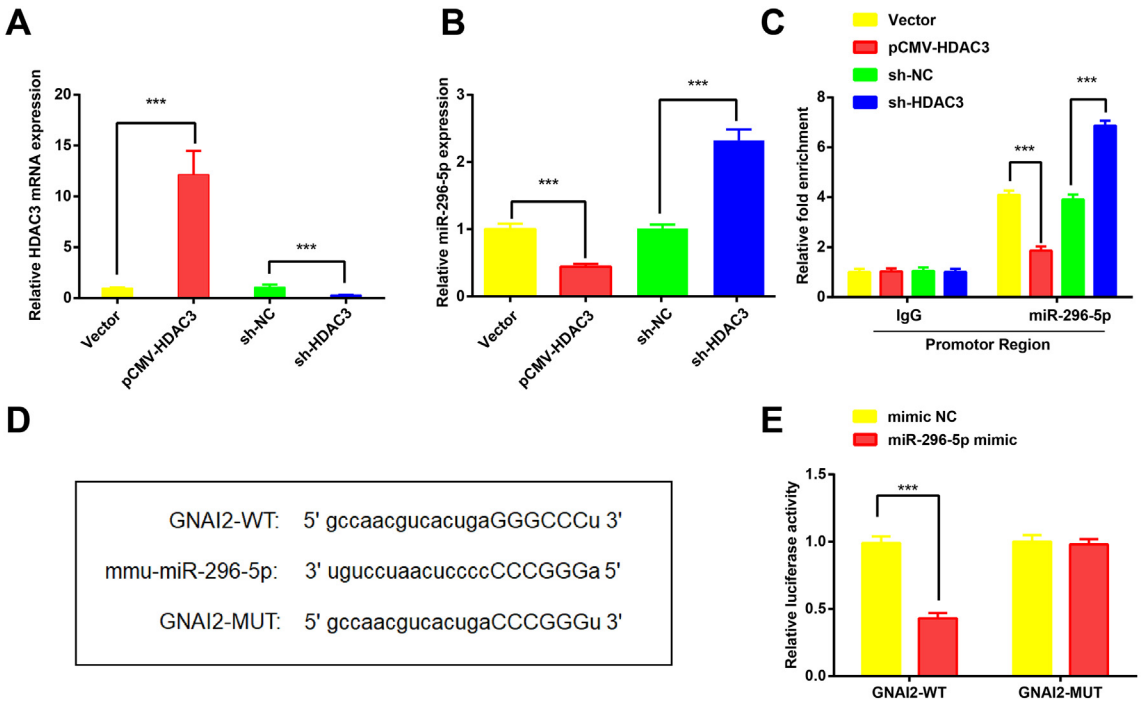


**Fig. 5.** HDAC3 targets miR-296-5p to modulate GNAI2 level. A. The expression of HDAC3 determined by RT-qPCR. B. The expression of miR-296-5p determined by RT-qPCR. C. The miR-296-5p promoter activity was examined by ChIP-qPCR. D, Prediction of the target relationship between miR-296-5p and GNAI2 by biological prediction. E, Dual luciferase reporter gene assay verified the target relationship of miR-296-5p and GNAI2. $^{**}P < 0.01$, $^{***}P < 0.001$. Measurement data were indicated as mean ± standard deviation. Comparisons between two groups were performed by *t*-test, and comparisons among multiple groups were assessed by ANOVA followed by Tukey's post hoc test. Cell experiment repeated at least three times independently.

rate, Bax and Caspase-3 expression, increased Bcl-2 expression, reduced VEGF and MDA contents, and enhanced SOD activity in serum and retinal tissues of DR mice. VEGF is an essential intermediary in neovascularization and permeability of the diabetic retina, and the elevated VEGF expression induces a reduction in the breakdown of the blood-retina barrier, an elevation in leukostasis within retinal vessels, as well as inflammation, all of which could contribute to DR pathology [37]. Also, there was increased content of MDA and decreased activity of SOD in retinas of diabetic rats versus the control rats [38]. Furthermore, glial cells in diabetic retinas express several antiapoptosis molecules, suggesting a possible effect of glial cells in the stimulation of apoptosis in ganglion cells [39]. Partly in line with our finding, it has been verified that up-regulation of miR-296-5p can reduce VEGF contents in thyroid cancer, and further hinder the aggressive biological behaviors of thyroid cancer after the interaction with its upstream gene [40]. It has been displayed that VEGF expression is markedly raised in DR rats [41]. A study has indicated that depletion of HDAC3 protects against cerebral I/R injury in the diabetic state *in vitro* and *in vivo* through the regulation of cell apoptosis [31]. Another study has presented that down-regulating HDAC3 triggers apoptosis in both patient multiple myeloma cells and MM cell lines [42].

In a word, our study provides evidence that depleting HDAC3 or restoring miR-296-5p hinders apoptosis of retinal ganglion cells of DR mice and dampens VEGF and MDA contents yet promoting SOD activities via down-regulating GNAI2 expression (Fig. 6). These findings furnish the target therapies for DR. Nevertheless, the exact functions of the HDAC3/miR-296-5p axis is not fully elucidated, and therefore, warrants future works.

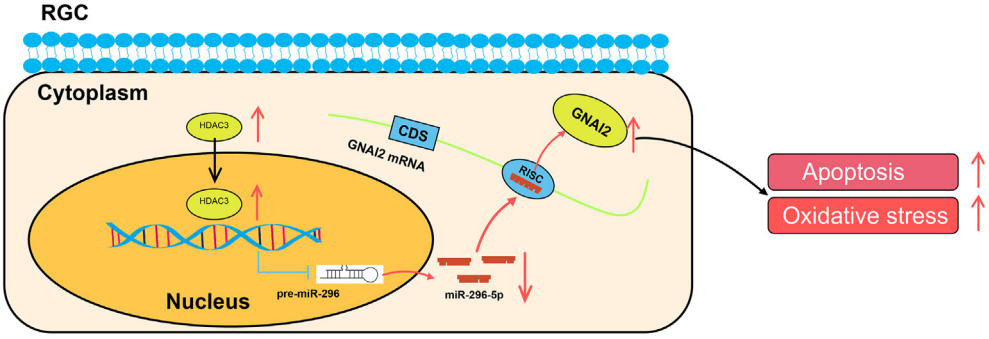


**Fig. 6.** The mechanistic diagram suggests that depleting HDAC3 or restoring miR-296-5p suppresses apoptosis of retinal ganglion cells of DR mice via down-regulating GNAI2.

## Declaration of competing interest

The authors declare no competing interests.

## Appendix A. Supplementary data

Supplementary data to this article can be found online at https://doi.org/10.1016/j.reth.2022.04.002.

## References


[1] Thomas AA, Biswas S, Chen S, Gonder J, Chakrabarti S. lncRNA H19 prevents endothelial-mesenchymal transition in diabetic retinopathy. Diabetologia 2019;62(3):517–30.
[2] Li S, Sun J, Liu Y, Lin D, Duan H, Liu F. The association of serum and vitreous adropin concentrations with diabetic retinopathy. Ann Clin Biochem 2019;56(2):253–8.
[3] Shaker OG, Abdelaleem OO, Mahmoud RH, Abdelghaffar NK, Ahmed TI, Said OM, et al. Diagnostic and prognostic role of serum miR-20b, miR-17-3p, HOTAIR, and MALAT1 in diabetic retinopathy. IUBMB Life 2019;71(3):310–20.
[4] Wang Y, Tao J, Jiang M, Yao Y. Apocynin ameliorates diabetic retinopathy in rats: involvement of TLR4/NF-kappaB signaling pathway. Int Immunopharmacol 2019;73:49–56.
[5] Duraisamy AJ, Mohammad G, Kowluru RA. Mitochondrial fusion and maintenance of mitochondrial homeostasis in diabetic retinopathy. Biochim Biophys Acta Mol Basis Dis 2019;1865(6):1617–26.
[6] Yin L, Sun Z, Ren Q, Su X, Zhang D. Long non-coding RNA BANCR is overexpressed in patients with diabetic retinopathy and promotes apoptosis of retinal pigment epithelial cells. Med Sci Monit 2019;25:2845–51.
[7] Choi YM, An S, Bae S, Jung JH. Mdm2 is required for HDAC3 monoubiquitination and stability. Biochem Biophys Res Commun 2019;517(2):353–8.
[8] Zhao Q, Zhang F, Yu Z, Guo S, Liu N, Jiang Y, et al. HDAC3 inhibition prevents blood-brain barrier permeability through Nrf2 activation in type 2 diabetes male mice. J Neuroinflammation 2019;16(1):103.
[9] Shan Q, Zheng G, Zhu A, Cao L, Lu J, Wu D, et al. Epigenetic modification of miR-10a regulates renal damage by targeting CREB1 in type 2 diabetes mellitus. Toxicol Appl Pharmacol 2016;306:134–43.
[10] Fu Y, Wang Y, Gao X, Li H, Yuan Y. Dynamic expression of HDAC3 in db/db mouse RGCs and its relationship with apoptosis and autophagy. J Diabetes Res 2020;2020:6086780.
[11] Shen X, Zhang X, Ru W, Huang Y, Lan X, Lei C, et al. circINSR promotes proliferation and reduces apoptosis of embryonic myoblasts by sponging miR-34a. Mol Ther Nucleic Acids 2020;19:986–99.
[12] Liu X, Wang Y, Zhang X, Zhang X, Guo J, Zhou J, et al. MicroRNA-296-5p promotes healing of diabetic wound by targeting sodium-glucose transporter 2 (SGLT2). Diabetes Metab Res Rev 2019;35(2):e3104.
[13] Favaro RR, Morales-Prieto DM, Herrmann J, Sonnemann J, Schleussner E, Markert UR, et al. Influence of high glucose in the expression of miRNAs and IGF1R signaling pathway in human myometrial explants. Arch Gynecol Obstet 2021;303(6):1513–22.
[14] Cao H, Qadri SM, Lang E, Pelzl L, Umbach AT, Leiss V, et al. Heterotrimeric G-protein subunit Galphai2 contributes to agonist-sensitive apoptosis and degranulation in murine platelets. Physiol Rep 2018;6(17):e13841.
[15] Li X, Zhang Y, Xia M, Gulbins E, Boini KM, Li PL. Activation of Nlrp3 inflammasomes enhances macrophage lipid-deposition and migration: implication of a novel role of inflammasome in atherogenesis. PLoS One 2014;9(1):e87552.
[16] Leiss V, Schönsiegel A, Gnad T, Kerner J, Kaur J, Sartorius T, et al. Lack of Galphai2 proteins in adipocytes attenuates diet-induced obesity. Mol Metab 2020;40:101029.
[17] Saddala MS, Lennikov A, Grab DJ, Liu GS, Tang S, Huang H. Proteomics reveals ablation of PlGF increases antioxidant and neuroprotective proteins in the diabetic mouse retina. Sci Rep 2018;8(1):16728.
[18] Zeng J, Xie X, Feng XL, Xu L, Han JB, Yu D, et al. Specific inhibition of the NLRP3 inflammasome suppresses immune overactivation and alleviates COVID-19 like pathology in mice. EBioMedicine 2022;75:103803.
[19] Zheng Y, Liu Y, Wang L, Xu H, Lu Z, Xuan Y, et al. MicroRNA126 suppresses the proliferation and migration of endothelial cells in experimental diabetic retinopathy by targeting pololike kinase 4. Int J Mol Med 2021;47(1):151–60.
[20] Ji Q, Han J, Wang L, Liu J, Dong Y, Zhu K, et al. MicroRNA-34a promotes apoptosis of retinal vascular endothelial cells by targeting SIRT1 in rats with diabetic retinopathy. Cell Cycle 2020;19(21):2886–96.
[21] Dong W, Chen Q, Zhao S, Wen S, Chen W, Ye W, et al. IKKalpha contributes to ischemia-induced autophagy after acute cerebral ischemic injury. Ann Transl Med 2022;10(4):160.
[22] Yu T, Liu D, Gao M, Yang P, Zhang M, Song F, et al. Dexmedetomidine prevents septic myocardial dysfunction in rats via activation of alpha7nAChR and PI3K/Akt- mediated autophagy. Biomed Pharmacother 2019;120:109231.
[23] Wang Y, Li Q, Niu L, Xu L, Guo Y, Wang L, et al. Suppression of G6PD induces the expression and bisecting GlcNAc-branched N-glycosylation of E-Cadherin to block epithelial-mesenchymal transition and lymphatic metastasis. Br J Cancer 2020;123(8):1315–25.
[24] Hu Q, Chen G, Yang Y, Xie H, Tian J. Histone deacetylase 3 aggravates type 1 diabetes mellitus by inhibiting lymphocyte apoptosis through the microRNA-296-5p/Bcl-xl Axis. Front Genet 2020;11:536854.
[25] Luo E, Wang D, Yang G, Qiao Y, Zhu B, Liu B, et al. The NF-kappaB/miR-425-5p/MCT4 axis: a novel insight into diabetes-induced endothelial dysfunction. Mol Cell Endocrinol 2020;500:110641.
[26] Naderi A, Zahed R, Aghajanpour L, Amoli FA, Lashay A. Long term features of diabetic retinopathy in streptozotocin-induced diabetic Wistar rats. Exp Eye Res 2019;184:213–20.
[27] Zhang J, Xu Z, Gu J, Jiang S, Liu Q, Zheng Y, et al. HDAC3 inhibition in diabetic mice may activate Nrf2 preventing diabetes-induced liver damage and FGF21 synthesis and secretion leading to aortic protection. Am J Physiol Endocrinol Metab 2018;315(2):E150–62.
[28] Platania CBM, Maisto R, Trotta MC, D'Amico M, Rossi S, Gesualdo C, et al. Retinal and circulating miRNA expression patterns in diabetic retinopathy: an in silico and in vivo approach. Br J Pharmacol 2019;176(13):2179–94.
[29] Zhang Y, Lv X, Hu Z, Ye X, Zheng X, Ding Y, et al. Protection of Mcc950 against high-glucose-induced human retinal endothelial cell dysfunction. Cell Death Dis 2017;8(7):e2941.
[30] Xu Z, Tong Q, Zhang Z, Wang S, Zheng Y, Liu Q, et al. Inhibition of HDAC3 prevents diabetic cardiomyopathy in OVE26 mice via epigenetic regulation of DUSP5-ERK1/2 pathway. Clin Sci (Lond) 2017;131(15):1841–57.
[31] Zhao B, Yuan Q, Hou JB, Xia ZY, Zhan LY, Li M, et al. Inhibition of HDAC3 ameliorates cerebral ischemia reperfusion injury in diabetic mice in vivo and in vitro. J Diabetes Res 2019;2019:8520856.
[32] Regmi A, Liu G, Zhong X, Hu S, Ma R, Hu L, et al. Evaluation of serum microRNAs in patients with diabetic kidney disease: a nested case-controlled study and bioinformatics analysis. Med Sci Monit 2019;25:1699–708.
[33] Chao ML, Luo S, Zhang C, Zhou X, Zhou M, Wang J, et al. S-nitrosylation-mediated coupling of G-protein alpha-2 with CXCR5 induces Hippo/YAP-dependent diabetes-accelerated atherosclerosis. Nat Commun 2021;12(1):4452.
[34] Tomita Y, Lee D, Miwa Y, Jiang X, Ohta M, Tsubota K, et al. Pemafibrate protects against retinal dysfunction in a murine model of diabetic retinopathy. Int J Mol Sci 2020;21(17).
[35] Zhu YN, Zuo GJ, Wang Q, Chen XM, Cheng JK, Zhang S. The involvement of the mGluR5-mediated JNK signaling pathway in rats with diabetic retinopathy. Int Ophthalmol 2019;39(10):2223–35.
[36] Ye Q, Lin YN, Xie MS, Yao YH, Tang SM, Huang Y, et al. Effects of etanercept on the apoptosis of ganglion cells and expression of Fas, TNF-alpha, caspase-8 in the retina of diabetic rats. Int J Ophthalmol 2019;12(7):1083–8.
[37] Yang F, Yu J, Ke F, Lan M, Li D, Tan K, et al. Curcumin alleviates diabetic retinopathy in experimental diabetic rats. Ophthalmic Res 2018;60(1):43–54.
[38] Chen F, Zhang HQ, Zhu J, Liu KY, Cheng H, Li GL, et al. Puerarin enhances superoxide dismutase activity and inhibits RAGE and VEGF expression in retinas of STZ-induced early diabetic rats. Asian Pac J Trop Med 2012;5(11):891–6.
[39] Abu-El-Asrar AM, Dralands L, Missotten L, Al-Jadaan IA, Geboes K. Expression of apoptosis markers in the retinas of human subjects with diabetes. Invest Ophthalmol Vis Sci 2004;45(8):2760–6.
[40] Chen Y, Gao H, Li Y. Inhibition of LncRNA FOXD3-AS1 suppresses the aggressive biological behaviors of thyroid cancer via elevating miR-296-5p and inactivating TGF-beta1/Smads signaling pathway. Mol Cell Endocrinol 2020;500:110634.
[41] Wu DM, Wen X, Wang YJ, Han XR, Wang S, Shen M, et al. Effect of microRNA-186 on oxidative stress injury of neuron by targeting interleukin 2 through the janus kinase-signal transducer and activator of transcription pathway in a rat model of Alzheimer's disease. J Cell Physiol 2018;233(12):9488–502.
[42] Harada T, Ohguchi H, Grondin Y, Kikuchi S, Sagawa M, Tai YT, et al. HDAC3 regulates DNMT1 expression in multiple myeloma: therapeutic implications. Leukemia 2017;31(12):2670–7.